

Modifications of Tanabe-Sugano d^6 diagram induced by radical ligand field: *ab initio* inspection of a Fe(II)-verdazyl molecular complex

Pablo Roseiro,[†] Saad Yalouz,^{*,†} David J. R. Brook,[‡] Nadia Ben Amor,[¶] and
Vincent Robert[†]

[†]*Laboratoire de Chimie Quantique, Institut de Chimie, CNRS/Université de Strasbourg, 4
rue Blaise Pascal, 67000 Strasbourg, France*

[‡]*Department of Chemistry, San José State University, One Washington Square, San José,
CA 95192, USA*

[¶]*Laboratoire de Physique et Chimie Quantiques, UMR 5626 Université Paul Sabatier, 118
route de Narbonne, 31062 Toulouse, France*

E-mail: yalouzsaad@gmail.com

Abstract

Quantum entanglement between the spin states of a metal centre and radical ligands is suggested in an iron(II) $[\text{Fe}(\text{dipyvd})_2]^{2+}$ compound (dipyvd = 1-isopropyl-3,5-dipyridil-6-oxoverdazyl). Wavefunction *ab initio* (Difference Dedicated Configuration Interaction, DDCI) inspections were carried out to stress the versatility of local spin states. We named this phenomenon *excited state spinmerism*, in reference to our previous work (see Roseiro et. al., ChemPhysChem 2022, e202200478) where we introduced the concept of spinmerism as an extension of mesomerism to spin degrees of freedom. The construction of localized molecular orbitals allows for a reading of the

wavefunctions and projections onto the local spin states. The low-energy spectrum is well-depicted by a Heisenberg picture. A 60 cm^{-1} ferromagnetic interaction is calculated between the radical ligands with the $S_{total} = 0$ and 1 states largely dominated by a local low-spin $S_{Fe} = 0$. In contrast, the higher-lying $S_{total} = 2$ states are superpositions of the local $S_{Fe} = 1$ (17%, 62%) and $S_{Fe} = 2$ (72%, 21%) spin states. Such mixing extends the traditional picture of a high-field d^6 Tanabe-Sugano diagram. Even in the absence of spin-orbit coupling, the avoided crossing between different local spin states is triggered by the field generated by radical ligands. This puzzling scenario emerges from versatile local spin states in compounds which extend the traditional views in molecular magnetism.

Introduction

The synthesis and characterization of molecule-based magnetic systems has been an intense research area for decades, prompted by the need for information storage devices and advances in quantum technologies (see for example Refs.^{1–4}). The motivations for targeting such complexes stem from their physical-chemical properties ranging from long coherence time^{5–9} to manipulation possibilities.^{10–15} In the presence of spin-switchable units, the local spin state of archetypical iron(II) or cobalt(II) ($3d^6$ and $3d^7$, respectively) ions can be controlled using external fields such as light or temperature. **Important structural modifications are observed along the $S_{total} = 0$ to $S_{total} = 2$ spin transition, with changes in bond distances of up to 0.2 Å (i.e. 10%).**¹⁶ Furthermore, *ab initio* calculations showed that this transition is not restricted to a mere change in the occupation numbers of the mostly d-type valence molecular orbitals (MOs). Indeed, deep changes in charge distribution (up to 0.5 electrons) were calculated between the iron(II) center and its coordination sphere.¹⁷ The latter are responsible for hysteretic behavior in materials¹⁸ and are known to be the main characteristic of valence tautomers.¹⁹ More recently, transition metal ions combined with organic ligands

have been considered as possible targets in the development of molecular-based quantum units of information, *e.g.* qubits or qudits (see for example Refs. ¹⁻⁴). Theoretical studies have also revealed the potential interest of radical ligands for the manipulation of quantum information via the entanglement of local spin degrees of freedom. ^{20,21} A prerequisite is the binding of radical ligands to paramagnetic metal centers without losing their open-shell character. In this respect, oxoverdazyl-based ligands have proven to fulfill such requirements, giving rise to a wealth of magnetic coupling schemes. ²²⁻²⁴ **Furthermore, the ease with which chemical modifications can be made and the well-established redox activity of organic-based compounds make such materials particularly interesting.** Not only can inter-unit interactions be modulated with speculated spin-crossover behaviour, ²⁵ but the field generated by several open-shell ligands may give rise to unusual and puzzling scenarios.

Recently, it has been suggested that the energy spectrum of a cobalt(II) ion coordinated to open-shell radicals may not be readily interpreted. **At the crossroads of exchange coupled and spin-crossover systems, the cobalt(II) oxoverdazyl compound $[\text{Co}(\text{dipyvd})_2]^{2+}$ (dipyvd=1- isopropyl-3,5-dipyridyl-6-oxoverdazyl) has questioned the traditional picture of a metal ion as either high-spin or low-spin, in the electrostatic field of neighbouring ligands.** ^{20,26} Wavefunction-based calculations supported that the spin states are characterized by combinations of various local spin states on the cobalt(II) center. In particular, the ground state displays a structure-sensitive admixture of low-spin $S_{Co} = 1/2$ in a dominant high-spin $S_{Co} = 3/2$, a feature of entanglement named *spinmerism*. The mixing was further interpreted by inspecting a d^7 Tanabe-Sugano diagram that exhibits a doublet-quartet crossing in the intermediate ligand field regime. *The spinmerism* phenomenon can be seen as an extension of mesomerism to spin degrees of freedom with entanglement in between two local sub-parts of a molecule. Since the ligand field includes Coulomb and direct exchange contributions in a complex built on spin-coupled partners, one may wonder whether different local spin states may coexist on the metal ion.

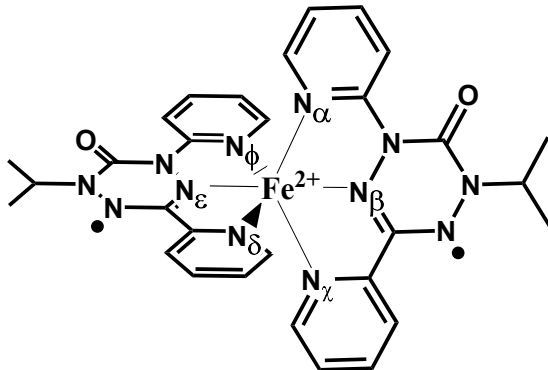


Figure 1: $[\text{Fe}(\text{dipyvd})_2]^{2+}$ compound (1) from Ref²⁷. The Xray Fe- N_i distances $i = \alpha - \phi$ are 1.98, 1.84, 1.95, 2.00, 1.85 and 1.98 Å, respectively.

The introduction of radical ligands may indeed disrupt the assumption of a given spin state on the metal centre in the description of ground and excited states.

Inspired by these observations, the pseudo-octahedral iron(II)-oxoverdazyl compound $[\text{Fe}(\text{dipyvd})_2]^{2+}$, with dipyvd = 1- isopropyl-3,5-dipyridil-6-oxoverdazyl (1) was considered as another prototype to be examined (see Figure 1).²⁷ Magnetic and spectroscopic properties were reported in the literature and complemented by density functional theory-based calculations suggesting a low-spin iron center.²⁷ **Bond lengths (for both ligand and metal ion) are characteristic of a low-spin iron(II) coordinated to neutral radical verdazyl ligands. In particular, the Fe-N bond distances were reported *ca.* 1.95 Å as mentioned in Figure 1. Such spin picture is also consistent with the IR spectrum, and the 5-300 K magnetic susceptibility measurements support a low-spin metal center.** Iron(II) being a spin-crossover metal ion, any intermediate ligand field should be appropriate to observe the coexistence of a $S_{\text{Fe}} = 0$ (low spin) and $S_{\text{Fe}} = 2$ (high spin). As seen in Figure 2, the d^6 Tanabe-Sugano diagram exhibits a crossing between the excited triplet and excited quintet states. Therefore, a similar manifestation of spin states mixing observed in the ground state of cobalt(II) complex might appear in the excited states of this iron(II) analogue. Guided by this observation in the high-field regime, we thought that *excited state spinmerism* might be anticipated, with total spin states resulting

from combinations of local $S_{Fe} = 1$ and $S_{Fe} = 2$. For all these reasons, *ab initio* calculations were carried out to inspect the energy spectrum of **1** (shown in Fig. 1), dominated by local spins modifications. The examined energy window consists of spin states characterized by similar charge distributions, leaving out ligand-to-metal and metal-to-ligand charge transfer states. The eigen-states were constructed using localized molecular orbitals (LMOs) to allow for projections onto the local spin states of the metal and ligands, S_{Fe} and S_L , respectively.

The numerical results presented in this work highlight the presence of a strong quantum entanglement between the local spin states, *i.e.* a *spinmerism* effect, of the metal ion and the radical ligand environment. This evidence reshuffles the standard views in molecular magnetism and simultaneously opens up new perspectives for technological development at the interface of physics and chemistry. **The traditional Tanabe-Sugano diagram concepts might be extended, giving possible out-of-the-box answers to energy spectra governed by ligand fields displaying open-shell character.** In Light-Induced Excited Spin-State Trapping (LIESST) experiments,²⁸ the long-lived excited states at low temperatures would consist of superpositions of $S_{Fe} = 1$ and $S_{Fe} = 2$. **Therefore, the variability of local spin states could provide a pathway to encode quantum information on synthetic molecular systems based on this light-induced qubit, presuming that the access to the different local S_{Fe} spin states is available (e.g. Fe-N bond stretching frequencies).**

Computational details

The presence of multiple open-shells on both metal ion and ligands strongly invites the use of a wavefunction-based method, such as the complete active space self-consistent field (CASSCF) method. The complete active space should include six electrons from the iron center and two from the oxoverdazyl ligands in seven molecular orbitals (CAS[8,7]). However, the active space was reduced to CAS[6,6] by inspecting the occupation numbers of

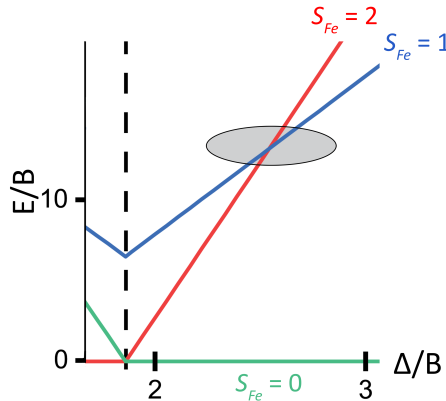


Figure 2: Low part of the Tanabe-Sugano diagram of an iron(II) d^6 ion in an octahedral field. The critical ligand field value marking spin-crossover is indicated by a vertical dotted line. The crossing between the excited $S_{Fe} = 1$ and $S_{Fe} = 2$ states is highlighted.

the active MOs. The CAS[6,6]SCF sextuplet MOs were then transformed into localized molecular orbitals (LMOs)²⁹ which are shown in Figure 3. Such transformation allows for a reading of the wavefunctions following a Lewis-like description. In the low-energy spectrum of **1**, we checked that the mostly metal d-type LMOs remained doubly occupied (low-spin iron(II)) and the active space was even reduced to CAS[2,2]. All CASSCF calculations were performed on the available Xray structure without any geometry optimization and used the MolCAS 8.0 package.³⁰ The iron and first coordination sphere atoms were described with 4s3p2d and 3s2p1d basis sets, respectively. Smaller basis sets 3s2p were used for all other atoms whilst hydrogen atoms were depicted with a 1s basis set. **Such basis set affords for a balanced description of the iron center and the first coordination sphere atoms fixing the crystal field amplitude. A similar basis set was previously used in the theoretical analysis of a cobalt(II) analogue.**²⁶ The dynamical correlation and polarization effects were included following the Difference Dedicated Configuration Interaction (DDCI) method^{31,32} as implemented in the CASDI code.³³ Given a set of MOs, the structures of the spin states can be directly compared from the CI amplitudes. Depending on the classes of excitations involved in the CI expansion, different levels (CAS + S, CAS +

DDC2 and CAS + DDCI) can be reached beyond the CAS pictures (CAS[2,2] or CAS[6,6]). This variational method that follows a step-by-step construction of the wavefunction has produced a wealth of interpretations and rationalizations with a systematic relaxation of the wavefunction (so-called "fully decontracted method"). The resulting CI eigenfunctions were projected onto the local spin states of the oxoverdazyl ligands pair ($S_L = 0$ or 1) and the iron ion ($S_{Fe} = 0, 1$ or 2). This procedure allows for a decomposition into the different entangled metal-ligand contributions. To implement these projections and conduct our local spin analysis, the open access package *QuantNBody*³⁴ was used. This numerical python toolbox has been recently developed by one of us (SY) to facilitate the manipulation of quantum many-body operators and wavefunctions. Based on this tool, matrix representations (in the many-electron basis) of the local metal and ligands spin operators \hat{S}_{Fe}^2 and \hat{S}_L^2 were built and diagonalized to access the local spin subspaces. This approach makes it possible to design spin projectors (in the many-electron basis) to target specific local spins contributions for the metal and the ligands in the multi-reference wavefunction.

Results and Discussion

First, CASSCF calculations were conducted on **1**. Inspections based on a CAS[8,7] highlight the presence of a MO mostly localized on a 3d iron atomic orbital with occupation number 1.99. Thus, the active space was reduced down to [6,6]. The CAS[6,6]SCF MOs were localized either on the metal center or on each individual dipyvd ligand (see Figure 3). Then, the electronic structure of the environment was inspected following the procedure recently developed on a $[\text{Co}(\text{dipyvd})_2]^{2+}$ compound (cobalt(II)).^{20,26} Based on a fictitious $[\text{Zn}(\text{dipyvd})_2]^{2+}$ (closed-shell divalent metal ion) analogue of the cobalt(II) compound, it was shown that the **singlet-triplet** energy difference $\mathbf{E}_S - \mathbf{E}_T$ is of the order of $+2 \text{ cm}^{-1}$.²⁰ Considering the geometry changes moving to compound **1**, a similar inspection was conducted by substituting iron(II) by zinc(II). A 1.9 cm^{-1} **singlet-triplet** energy difference was computed at the

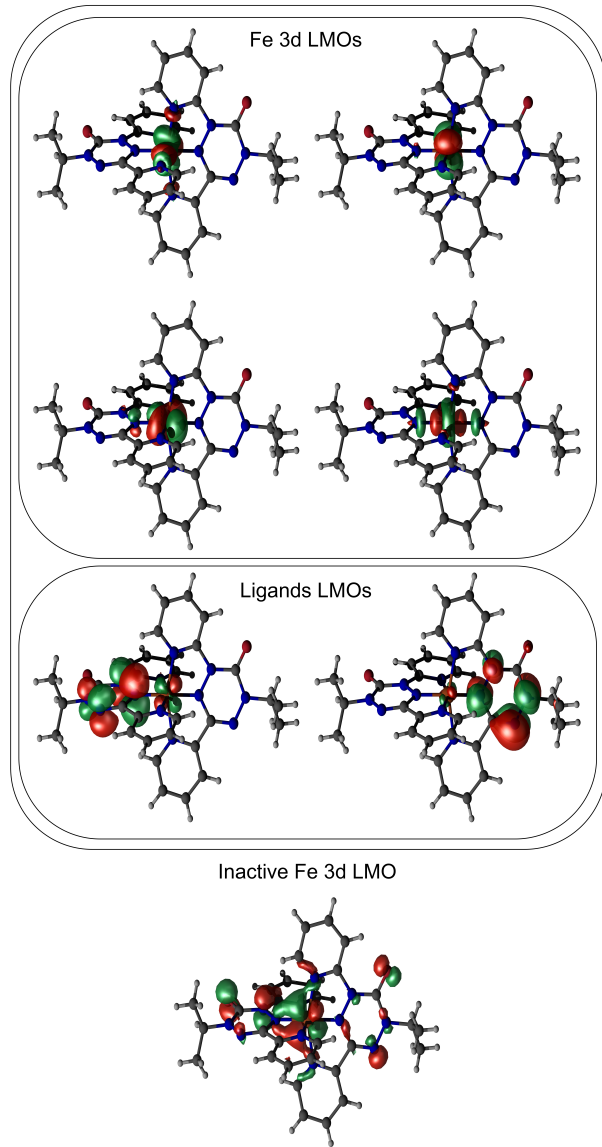


Figure 3: Representations of the four mostly metal-type and the two mostly ligand-type LMOs included in the CAS[6,6] generated from a CAS[8,7]SCF calculation for the sextuplet spin state of 1. The mostly 3d-type inactive LMO is shown below.

CAS[2,2] + DDCI level. This negligible exchange coupling value between the radical ligands suggests that any projection of the total spin states of **1** may simultaneously involve the local $S_L = 0$ and $S_L = 1$ states. Besides, this value can be seen as a reference to quantify the role of the electronic structure of the bridging metal ion. Indeed, the nature, and more importantly the spin state, of the metal center are likely to modify the exchange coupling constant value, a particular issue we wanted to inspect. As reported in the literature, the intramolecular radical-radical exchange couplings were measured in a series of M(II)-(bipyvdz)₂ complexes (M = Mn, Ni, Cu, Zn) and range from weakly antiferromagnetic (-10 cm^{-1}) to weakly ferromagnetic ($+2\text{ cm}^{-1}$).²⁴ Due to the system size and the number of open-shells, a CAS[6,6] + DDCI level of calculation is out of reach. Thus, all our conclusions are based on CAS[6,6] + DDC2 excitation energies and corresponding wavefunctions analysis, as summarized in Table 1.

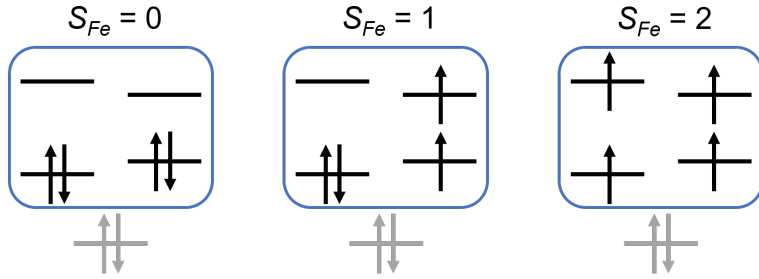
The energy spectrum results from the local spin states $S_{Fe} = 0, 1, 2$ and $S_L = 0, 1$ which give rise to ten states, namely two singlets ($S_i, i = 0 - 1$), four triplets ($T_i, i = 0 - 3$), three quintets ($Q_i, i = 0 - 2$) and a single heptuplet (H_0). From our calculations, the local spin states display 0, 2 and 4 open-shells on the $S_{Fe} = 0$, $S_{Fe} = 1$ and $S_{Fe} = 2$, respectively (see Scheme 1). **One should stress that the local $S_{Fe} = 1$ spin state involves a single pair of LMOs, a manifestation of the absence of orbital degeneracy as schematically shown in Scheme 1.** The local spin values can result either from pure spin states or superpositions of different spin multiplicities as manifested in spinmerism.^{20,21} Therefore, four different classes can be *a priori* anticipated in the energy spectrum of **1**.

Let us concentrate on the first class of states dominated by pure local spin states S_{Fe} and S_L (see light grey (\star) entry in Table 1). First, the ground state T_0 is triplet, dominated by the local spin states $S_{Fe} = 0$ and $S_L = 1$, respectively, followed by the singlet S_0 lying 120 cm^{-1} above. This picture is consistent with a d^6 low-spin metal ion in a high-field environment. One should note that small admixtures (13 – 16%) of charge transfers ($S_{Fe} = 1/2$ and $S_L = 1/2$) are evidently observed. Since the CAS[6,6]SCF occupation numbers of the mostly

Table 1: Energy spectrum of **1**. Quintets and heptuplet energies are calculated at the CAS[6,6] + DDC2 level. The ground state energy is used as a reference energy. The spin multiplicities $2S_{total} + 1$ and $S_{Fe} \otimes S_L$ decompositions of the wavefunctions are given on the local spin states S_{Fe} and S_L . S , T , Q and H correspond to singlet, triplet, quintet and heptuplet, respectively. The \star symbol is used to refer to states consisting of pure local spin states on both metal and ligand centers. The \bullet symbol refers to states consisting of pure local spin states on the metal center, and mixed spin values on the ligands. Spin states consisting of mixed spin values on both metal and ligands do not show any symbol, and are manifestation of excited state spinmerism.

| Label | Energy (cm^{-1}) | $2S_{total} + 1$ | $S_{Fe} \otimes S_L$ | |
|-------|-------------------------|------------------|----------------------|--|
| Q_2 | • | 10156 | 5 | 86% Q 42% S 44% T |
| S_1 | ★ | 8603 | 1 | 82% T 82% T |
| T_3 | ★ | 7691 | 3 | 83% Q 83% T |
| T_2 | • | 6705 | 3 | 87% T 9% S 78% T |
| H_0 | ★ | 5326 | 7 | 100% Q 100% T |
| T_1 | • | 4972 | 3 | 81% T 78% S 3% T |
| Q_1 | | 3323 | 5 | 11% Q 10% Q 62% T 11% S 10% T 62% T |
| Q_0 | | 2906 | 5 | 39% Q 33% Q 17% T 39% S 33% T 17% T |
| S_0 | ★ | 120 | 1 | 84% S 84% S |
| T_0 | ★ | 0 (ref.) | 3 | 87% S 87% T |

d-type LMOs are larger than 1.98, the $S_0 - T_0$ energy difference was further confirmed from CAS[2,2] + DDCI calculations (CAS[2,2]SCF triplet MOs) and turned out to be 120 cm^{-1} . This value is in reasonable agreement with the reported one which may vary depending on the extraction from density functional theory broken-symmetry calculations.²⁷ Thus, the low-energy part of the spectrum of **1** can be viewed as two organic radicals coupled through a closed-shell iron(II) (see Figure 4). Evidently, a Heisenberg Hamiltonian $\hat{H} = -2J\hat{s}_1\hat{s}_2$ can be derived from the singlet-triplet energy difference. **The calculated ferromagnetic exchange coupling constant $J = +60\text{ cm}^{-1}$ is consistent with the experimental**



Scheme 1: **Schematic representations of the leading electronic configurations on the iron(II) center, whatever the total spin state in the energy spectrum of 1.** A single mostly d-type LMO which remains essentially doubly occupied (inactive) is shown below. For the sake of simplicity, the maximum spin projections on the local S_{Fe} spin states are shown.

value extracted from the magnetic susceptibility fitting ($+82 \text{ cm}^{-1}$).²⁷ This coupling is significantly larger than the reference one we estimated to be $+0.95 \text{ cm}^{-1}$ for the closed-shell hypothetical zinc(II) complex. **The filling of the mostly 3d type e_g -orbitals moving from iron(II) (d^6 ion) to zinc(II) (d^{10} ion) deeply modifies the electronic structure of the bridging unit (*i.e.*, the metal ion).** Similar to the effect of structural modification, such substitution is likely to alter the exchange mechanism **between the two verdazyl spin holders and its impact is difficult to anticipate.**

Such contrast is also found with the experimental values reported in a series of compounds, that not only differ from the relative positions of the verdazyl ligands but also from the absence of the iron(II) complex in the series.²⁴ The higher-lying states T_3 , S_1 (and evidently the heptuplet H_0) are all characterized by a pure $S_L = 1$ spin state on the coordination sphere. These states are expected from the traditional d^6 Tanabe-Sugano diagram (see Figure 2). In a triplet $S_L = 1$ high-field regime, the states ordering follows $S_{Fe} = 0$ (T_0 , reference energy), $S_{Fe} = 2$ (T_3 , 7691 cm^{-1}), and $S_{Fe} = 1$ (S_1 , 8603 cm^{-1}). At this stage, the main difference with usual picture in coordination chemistry compounds lies in the triplet nature of the ligand field, a concept introduced in the literature as "excited state coordination chemistry".³⁵ One should finally mention the presence of 1.6% singlet state on the metal in S_1 . However, this negligible contribution arises from an excited open-shell singlet.

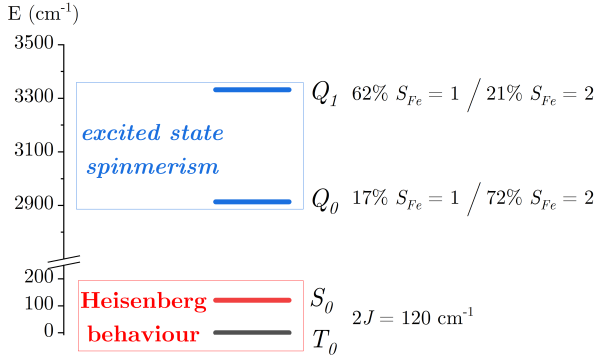


Figure 4: **Energy spectrum of **1** reflecting a Heisenberg behaviour in the low-energy part with T_0 and S_0 states, whereas *excited state spinmerism* is observed higher in energy with Q_0 and Q_1 states.** The excited quintet states Q_0 and Q_1 exhibit a strong mixing between the $S_{Fe} = 1$ and $S_{Fe} = 2$ local spin states.

Based on this preliminary observation suggesting a $S_L = 1$ ligand field, we now examine the third Q_1 ($2S_{total} + 1 = 5$) excited state given in Table 1. The iron(II) spin state is dominated by a $S_{Fe} = 1$ (62%) in the field of a 72% $S_L = 1$. Again, such picture obtained from the spin projections of the wavefunction is consistent with a high-field d^6 Tanabe-Sugano diagram.³⁶ However, the quintet state Q_1 in Figure 4 exhibits non-negligible contributions from the local $S_{Fe} = 2$ (21%) and $S_L = 0$ (11%) spin states. Such superposition of triplet and quintet metal spin states in the absence of spin-orbit coupling is a manifestation of the recently reported *spinmerism* effect.²⁰ Our analysis supports the appearance of a similar phenomenon in **1**, named as *excited state spinmerism*. This manifestation results from the open-shell character of the environment and the energy crossing between the $S_{Fe} = 1$ and $S_{Fe} = 2$ excited states in the high-field regime of the iron(II) d^6 diagram (see Figure 2). The traditional allowed crossing between different spin multiplicities in the Tanabe-Sugano diagram is lifted from the presence of two radical ligands. As expected, the energy spectrum exhibits a second close-in-energy quintet state resulting from this mixing (see Q_0 in Figure 4). The latter is found 2906 cm^{-1} above the ground state, with a dominant $S_{Fe} = 2$ character (72%), and a significant mixing between the environment $S_L = 0$ (39%) and $S_L = 1$ (50%) spin states. This second class of states (Q_0 and Q_1 in Table 1) displays entanglement

between the spin states of the metal ion and its coordination sphere in the high-field regime. In agreement with a recent inspection based on a model Hamiltonian²¹, the emergence of the two quintet states Q_0 and Q_1 in Figure 4 from avoided crossing stresses the importance of not only the magnitude of the ligand field (Coulomb contributions), but also the open-shell character of such field (decisive exchange contributions).

From these numerical inspections, one may further take advantage of the electronic structure changes observed in the photo-induced spin-states of spin crossover compounds (LIESST effect). Under low-temperature irradiation, it is possible to quantitatively achieve a low-spin to high-spin conversion in iron(II) spin-crossover compounds.²⁸ Very recently, it has been shown that unusually long relaxation times can be reached (*ca.* 20 hours) which makes such complexes particularly encouraging for practical applications.³⁷ **Starting from the ground state T_0 in compound 1, the spin-allowed transition would lead to the photo-generated T_1 state dominated by a local $S_{Fe} = 1$. The Q_1 state, and to a lesser extent the Q_0 state, exhibit a large proportion of the $S_{Fe} = 1$ local state (62% in Table 1). Thus, one may question whether intersystem crossing between T_1 and Q_1 would be enhanced by the presence of excited state spinermism.** The mechanism of light-induced spin crossover was previously studied to calculate intersystem-crossing rates and concluded on a process mediated by a triplet excited state.^{38,39} From the manifestation of the here-proposed *excited state spinermism* phenomenon, the LIESST effect would produce local superpositions of iron(II) spin states with potential applications as spin-qubits.

A third class of states in the energy spectrum of **1** is characterized by a pure local spin state on the metal and a superposition of $S_L = 0$ and $S_L = 1$ on the environment (T_1 , T_2 , Q_2 , see dark grey entry (\bullet) in Table 1). Such mixture was previously reported in noninnocent ligand-based iron(III) compounds^{40,41} where the "excited state coordination chemistry" concept³⁵ was numerically evidenced. In compound **1**, charge transfers are small enough to maintain a formally iron(II) ion with spin crossover behavior, a prerequisite for

spinmerism manifestation.

Finally, our analysis of the low-lying spin states does not reflect any representative of the fourth class, characterized by the superposition of S_{Fe} values in the field of a pure S_L value. Evidently, a $S_L = 0$ ligand field would not allow the mixing of different S_{Fe} values. However, the absence of a mixed-spin state on the metal in a $S_L = 1$ ligand field is more puzzling at first. As recently reported, the entanglement between local spin states is directly controlled by the relative amplitudes of the direct exchange values and conditions which might not be fulfilled in the examined compound **1**.²¹

Conclusion

The spin states structures of a coordination compound $[\text{Fe}(\text{dipvdz})_2]^{2+}$ built on a spin-crossover ion (iron(II)) and two radical ligands (oxoverdazyl) were analyzed from DDCI wavefunctions calculations. The procedure is based on the generation of localized molecular orbitals and spin projections onto the local spin states. A ground state triplet $S_{total} = 1$ characterized by a $S_{Fe} = 0$ local spin state is found, a reflection of a high-field regime. A strong ferromagnetic interaction $J = +60 \text{ cm}^{-1}$ is calculated featuring the coupling of organic radical spin holders through a low-spin metal ion. Even though the low-energy part of the spectrum can be rationalized by a Heisenberg spin Hamiltonian, the magnetic picture delivered by a d^6 Tanabe-Sugano diagram is deeply reshuffled in the next nearest excited states. The flexibility afforded by the open-shell character of the environment gives rise to marked superpositions of local spin states $S_{Fe} = 1$ and $S_{Fe} = 2$ in the $S_{total} = 2$ excited states. The traditional quasi-degeneracy in the high-field regime is lifted by 417 cm^{-1} with significant contributions from both $S_L = 1$ and $S_L = 0$ on the ligand pair. This observation, which we name *excited state spinmerism*, extends a phenomenon that was reported in a cobalt(II) analogue. The prerequisite for the manifestation of such entanglement is fulfilled from the presence of an iron(II) ion and radical organic ligands. By irradiating the sample

in the UV-vis or near-IR regions at low temperature, such compounds might be photo-switched and become original targets. Our analysis may stimulate experimentalists to photo-generate slowly decaying excited states consisting of $S_{Fe} = 1$ and $S_{Fe} = 2$ spin states superpositions. **Assuming that one can access the proportions of the different local S_{Fe} spin states, the reading of encoded quantum information may become feasible.** Therefore, the variability of local spin states could provide a pathway to encode quantum information on synthetic molecular systems. This particular class of coordination chemistry compounds combining versatile local spin states not only enlarges the traditional pictures in molecular magnetism but might become original targets for spin-qubit generation.

Acknowledgements

This work was supported by the Interdisciplinary Thematic Institute SysChem via the IdEx Unistra (ANR-10-IDEX-0002) within the program Investissement d’Avenir. P. R. acknowledges the Ecole Doctorale de Sciences Chimiques de Strasbourg, EDSC222, and the french minister for financial support. D.J.R.B acknowledges the support of the National Science Foundation Grant CHE-1900491. The authors would like to thank Pr. C. Train, Dr. G. Novitchi and Dr. S. Stoian for useful discussions.

AUTHOR DECLARATIONS

CONFLICTS OF INTEREST

The authors have no conflicts to disclose.

DATA AVAILABILITY

The data that support the findings of this study are available from the corresponding author upon reasonable request.

References

- (1) Gaita-Ariño, A.; Luis, F.; Hill, S.; Coronado, E. Molecular spins for quantum computation. *Nature chemistry* **2019**, *11*, 301–309.
- (2) Troiani, F.; Affronte, M. Molecular spins for quantum information technologies. *Chemical Society Reviews* **2011**, *40*, 3119–3129.
- (3) Stamp, P. C.; Gaita-Arino, A. Spin-based quantum computers made by chemistry: hows and whys. *Journal of Materials Chemistry* **2009**, *19*, 1718–1730.
- (4) McAdams, S. G.; Ariciu, A.-M.; Kostopoulos, A. K.; Walsh, J. P.; Tuna, F. Molecular single-ion magnets based on lanthanides and actinides: Design considerations and new advances in the context of quantum technologies. *Coordination Chemistry Reviews* **2017**, *346*, 216–239.
- (5) Atzori, M.; Morra, E.; Tesi, L.; Albino, A.; Chiesa, M.; Sorace, L.; Sessoli, R. Quantum coherence times enhancement in vanadium (IV)-based potential molecular qubits: the key role of the vanadyl moiety. *Journal of the American Chemical Society* **2016**, *138*, 11234–11244.
- (6) Atzori, M.; Tesi, L.; Morra, E.; Chiesa, M.; Sorace, L.; Sessoli, R. Room-temperature quantum coherence and rabi oscillations in vanadyl phthalocyanine: toward multifunctional molecular spin qubits. *Journal of the American Chemical Society* **2016**, *138*, 2154–2157.
- (7) Bader, K.; Dengler, D.; Lenz, S.; Endeward, B.; Jiang, S.-D.; Neugebauer, P.; Van Slageren, J. Room temperature quantum coherence in a potential molecular qubit. *Nature Communications* **2014**, *5*, 1–5.
- (8) Graham, M. J.; Zadrozny, J. M.; Shiddiq, M.; Anderson, J. S.; Fataftah, M. S.; Hill, S.; Freedman, D. E. Influence of electronic spin and spin–orbit coupling on decoherence

in mononuclear transition metal complexes. *Journal of the American Chemical Society* **2014**, *136*, 7623–7626.

(9) Atzori, M.; Benci, S.; Morra, E.; Tesi, L.; Chiesa, M.; Torre, R.; Sorace, L.; Sessoli, R. Structural effects on the spin dynamics of potential molecular qubits. *Inorganic Chemistry* **2018**, *57*, 731–740.

(10) Bayliss, S.; Laorenza, D.; Mintun, P.; Kovos, B.; Freedman, D. E.; Awschalom, D. Optically addressable molecular spins for quantum information processing. *Science* **2020**, *370*, 1309–1312.

(11) Carretta, S.; Zueco, D.; Chiesa, A.; Gómez-León, Á.; Luis, F. A perspective on scaling up quantum computation with molecular spins. *Applied Physics Letter* **2021**, *118*, 240501.

(12) Li, J.; Xiong, S.-J.; Li, C.; Jin, B.; Zhang, Y.-Q.; Jiang, S.-D.; Ouyang, Z.-W.; Wang, Z.; Wu, X.-L.; van Tol, J., et al. Manipulation of Molecular Qubits by Isotope Effect on Spin Dynamics. *CCS Chemistry* **2021**, *3*, 2548–2556.

(13) Nelson, J. N.; Zhang, J.; Zhou, J.; Rugg, B. K.; Krzyaniak, M. D.; Wasielewski, M. R. CNOT gate operation on a photogenerated molecular electron spin-qubit pair. *Journal of Chemical Physics* **2020**, *152*, 014503.

(14) Thiele, S.; Balestro, F.; Ballou, R.; Klyatskaya, S.; Ruben, M.; Wernsdorfer, W. Electrically driven nuclear spin resonance in single-molecule magnets. *Science* **2014**, *344*, 1135–1138.

(15) Hussain, R.; Allodi, G.; Chiesa, A.; Garlatti, E.; Mitcov, D.; Konstantatos, A.; Pedersen, K. S.; De Renzi, R.; Piligkos, S.; Carretta, S. Coherent manipulation of a molecular Ln-based nuclear qudit coupled to an electron qubit. *Journal of the American Chemical Society* **2018**, *140*, 9814–9818.

(16) Hauser, A. In *Spin Crossover in Transition Metal Compounds I*; Gütlich, P., Goodwin, H., Eds.; Springer Berlin Heidelberg: Berlin, Heidelberg, 2004; pp 49–58.

(17) Kepenekian, M.; Le Guennic, B.; Robert, V. Primary Role of the Electrostatic Contributions in a Rational Growth of Hysteresis Loop in Spin-Crossover Fe(II) Complexes. *Journal of the American Chemical Society* **2009**, *131*, 11498–11502.

(18) Kepenekian, M.; Le Guennic, B.; Robert, V. Magnetic bistability: From microscopic to macroscopic understandings of hysteretic behavior using ab initio calculations. *Physical Review B* **2009**, *79*, 094428.

(19) Tezgerevska, T.; Alley, K. G.; Boskovic, C. Valence tautomerism in metal complexes: Stimulated and reversible intramolecular electron transfer between metal centers and organic ligands. *Coordination Chemistry Reviews* **2014**, *268*, 23–40.

(20) Roseiro, P.; Ben Amor, N.; Robert, V. Combining Open-Shell Verdagyl Environment and Co(II) Spin-Crossover: Spinmerism in Cobalt Oxoverdagyl Compound. *ChemPhysChem* **2022**, *23*, e202100801.

(21) Roseiro, P.; Petit, L.; Robert, V.; Yalouz, S. Emergence of Spinmerism for Molecular Spin-Qubits Generation. *ChemPhysChem* **2022**, e202200478.

(22) Oms, O.; Rota, J.-B.; Norel, L.; Calzado, C. J.; Rousselière, H.; Train, C.; Robert, V. Beyond Kahn’s Model: Substituent and Heteroatom Influence on Exchange Interaction in a Metal-Verdagyl Complex. *European Journal of Inorganic Chemistry* **2010**, *2010*, 5373–5378.

(23) Brook, D. J. R.; Richardson, C. J.; Haller, B. C.; Hundley, M.; Yee, G. T. Strong ferromagnetic metal–ligand exchange in a nickel bis(3,5-dipyridylverdagyl) complex. *Chem. Commun.* **2010**, *46*, 6590–6592.

(24) Barclay, T. M.; Hicks, R. G.; Lemaire, M. T.; Thompson, L. K. Verdagyl Radicals as Oligopyridine Mimics: Structures and Magnetic Properties of M(II) Complexes of 1,5-Dimethyl-3-(2,2'-bipyridin-6-yl)-6-oxoverdagyl (M = Mn, Ni, Cu, Zn). *Inorganic Chemistry* **2003**, *42*, 2261–2267.

(25) Rota, J.-B.; Le Guennic, B.; Robert, V. Toward Verdagyl Radical-Based Materials: Ab Initio Inspection of Potential Organic Candidates for Spin-Crossover Phenomenon. *Inorganic Chemistry* **2010**, *49*, 1230–1237.

(26) Fleming, C.; Chung, D.; Ponce, S.; Brook, D. J. R.; DaRos, J.; Das, R.; Ozarowski, A.; Stoian, S. A. Valence tautomerism in a cobalt-verdagyl coordination compound. *Chem. Commun.* **2020**, *56*, 4400–4403.

(27) Brook, D. J. R.; Fleming, C.; Chung, D.; Richardson, C.; Ponce, S.; Das, R.; Srikanth, H.; Heindl, R.; Noll, B. C. An electron transfer driven magnetic switch: ferromagnetic exchange and spin delocalization in iron verdazyl complexes. *Dalton Trans.* **2018**, *47*, 6351–6360.

(28) Decurtins, S.; Gütlich, P.; Köhler, C.; Spiering, H.; Hauser, A. Light-induced excited spin state trapping in a transition-metal complex: The hexa-1-propyltetrazole-iron (II) tetrafluoroborate spin-crossover system. *Chemical Physics Letters* **1984**, *105*, 1–4.

(29) Maynau, D.; Evangelisti, S.; Guihéry, N.; Calzado, C. J.; Malrieu, J.-P. Direct generation of local orbitals for multireference treatment and subsequent uses for the calculation of the correlation energy. *The Journal of Chemical Physics* **2002**, *116*, 10060–10068.

(30) Aquilante, F. et al. Molcas 8: New capabilities for multiconfigurational quantum chemical calculations across the periodic table. *Journal of Computational Chemistry* **2016**, *37*, 506–541.

(31) Miralles, J.; Daudey, J.-P.; Caballol, R. Variational calculation of small energy dif-

ferences. The singlet-triplet gap in $[\text{Cu}_2\text{Cl}_6]^{2-}$. *Chemical physics letters* **1992**, *198*, 555–562.

(32) Miralles, J.; Castell, O.; Caballol, R.; Malrieu, J.-P. Specific CI calculation of energy differences: Transition energies and bond energies. *Chemical physics* **1993**, *172*, 33–43.

(33) Ben Amor, N.; Maynau, D. Size-consistent self-consistent configuration interaction from a complete active space. *Chemical Physics Letters* **1998**, *286*, 211–220.

(34) Yalouz, S.; Gullin, M. R.; Sekaran, S. QuantNBody: a Python package for quantum chemistry and physics to build and manipulate many-body operators and wave functions. *Journal of Open Source Software* **2022**, *7*, 4759.

(35) Ghosh, P.; Bill, E.; Weyhermüller, T.; Neese, F.; Wieghardt, K. Noninnocence of the Ligand Glyoxal-bis (2-mercaptoanil). The Electronic Structures of $[\text{Fe}(\text{gma})]_2$, $[\text{Fe}(\text{gma})(\text{py})]$, $[\text{Fe}(\text{gma})(\text{CN})]_1$, $[\text{Fe}(\text{gma})_2]$, and $[\text{Fe}(\text{gma})(\text{PR}_3)_n]$ ($n = 1, 2$). Experimental and Theoretical Evidence for “Excited State” Coordination. *Journal of the American Chemical Society* **2003**, *125*, 1293–1308.

(36) Tanabe, Y.; Sugano, S. On the Absorption Spectra of Complex Ions II. *Journal of the Physical Society of Japan* **1954**, *9*, 766–779.

(37) Delgado, T.; Tissot, A.; Guénée, L.; Hauser, A.; Valverde-Muñoz, F. J.; Seredyuk, M.; Real, J. A.; Pillet, S.; Bendeif, E.-E.; Besnard, C. Very Long-Lived Photogenerated High-Spin Phase of a Multistable Spin-Crossover Molecular Material. *Journal of the American Chemical Society* **2018**, *140*, 12870–12876.

(38) Sousa, C.; deGraaf, C.; Rudavskyi, A.; Broer, R.; Tatchen, J.; Etinski, M.; Marian, C. M. Ultrafast Deactivation Mechanism of the Excited Singlet in the Light-Induced Spin Crossover of $[\text{Fe}(2,2\text{-bipyridine})_3]^{2+}$. *Chemistry – A European Journal* **2013**, *19*, 17541–17551.

(39) Alías-Rodríguez, M.; Huix-Rotllant, M.; de Graaf, C. Quantum dynamics simulations of the thermal and light-induced high-spin to low-spin relaxation in Fe(bpy)3 and Fe(mtz)6. *Faraday Discuss.* **2022**, *237*, 93–107.

(40) Messaoudi, S.; Robert, V.; Guihéry, N.; Maynau, D. Correlated ab Initio Study of the Excited State of the Iron-Coordinated-Mode Noninnocent Glyoxalbis(mercaptoanil) Ligand. *Inorganic Chemistry* **2006**, *45*, 3212–3216, PMID: 16602777.

(41) Guihéry, N.; Robert, V.; Neese, F. Ab Initio Study of Intriguing Coordination Complexes: A Metal Field Theory Picture. *The Journal of Physical Chemistry A* **2008**, *112*, 12975–12979, PMID: 18811129.